# Thermal state of the crustal lithosphere and the mantle of Patagonia

Carlos Henrique Alexandrino[1], Carlos Alberto Mirez Tarrillo[1], André Froede Silva[1], Juliana de Oliveira Batista[1], Carlos Eduardo Cardoso Nogueira[1]
[1] Federal University of the Jequitinhonha and Mucury Valleys, Teófilo Otoni - MG, Brazil



## Abstract

Crustal thermal models that incorporate thermo-barometric data have been developed for estimating depth to 1300ºC isotherm in three xenoliths provinces of southern Patagonia (Argentina). Uncertainties in model results can be minimized by imposing reasonable bounds on some of the key model parameters. Experimental mineral temperature data indicates ranges of 877 to 1253ºC for the Rio Negro province and 728 to 1196ºC for the Santa Cruz province. Santa Cruz province has the highest heat flow (85±5 $mWm^{-2}$) at the surface and also the highest temperature (760±45ºC) at Moho's depth, Río Negro province has the lowest thermal thickness value (75±11 km) and the highest heat flow (44± $mWm^{-2}$) at Moho depth, this indicates that there are possibly two plumes heads responsible for xenoliths deposition in the region: one in Río Negro province and another in Santa Cruz. Analyzing only the best fit results we can infer average values for geothermal parameters at the surface: heat flow 81 $mWm^{-2}$, radiogenic heat production 1.4 $\mu Wm^{-3}$ at Moho depth: heat flow 40 $mWm^{-2}$, radiogenic heat production $2x10^{-2}$ $\mu Wm^{-3}$ and temperature 734ºC. Thermal thickness 81km and coefficient of variation of thermal conductivity with temperature $2x10^{-4}$ W $m^{-1}$ $ºC^{-2}$.

**Keywords:**. Xenoliths Provinces, Patagonia (Argentina), Radiogenic heat, Heat flow

## 1. Introduction

Ultramafic xenoliths (peridotite-pyroxenites) and eclogitic minerals present in intrusive rocks such as kimberlites. Lamproites and alkaline basalts are widely used to infer the temperature and pressure of the upper mantle and lower crust (Kukkonen and Peltonen, 1999; Russell and Kopylova, 1999; Russell et al., 2001; Harder and Russell, 2006; Aulbach et al., 2004; Howarth et al., 2014; Dymshits et al., 2020) as xenoliths preserve their physical and chemical characteristics while being transported by magmatic processes. Thus the method of estimating the thermal field using the thermo-barometric equilibrium condition of xenoliths has become an important means of estimating the thermal regime of the lithosphere for estimating the thermal regime of the lithosphere.

The method was used by Rudnick et al., (1998) in a global study with the purpose of investigating the thermal regime in Archaean terrains Russell et al., (2001) evaluated radiogenic heat production and basal heat flow in the Slave Craton region of Canada via thermo-barometrical xenoliths data. A similar method also was used by Dymshits et al., (2020) to estimate the thermal state, thickness and composition of the Siberian Craton. These studies show that the information extracted via equilibrium conditions from samples of xenoliths of man-made origin constitutes an efficient way to infer geothermal parameters in the lithosphere, especially in the upper mantle and lower crust.

In this context, the region of Patagonia in Argentina provides an opportunity to infer geothermal parameters. at Moho's depth being covered by geologically recent basaltic volcanism it provides samples of ultramafic xenoliths directly from the upper mantle from data compiled in works published in the past two decades (Mallmann, 2004; Bjerg et al., 2005; Ntaflos et al., 2007; Rieck et al., 2007; Schilling et al., 2017 and references therein).

Therefore the objective of our study is usefulness of the information of temperature and pressure of mineralogical balance of the to estimate the thermal state of the crustal lithosphere and the mantle.

## 2. Geologic Setting

The regional geology of Patagonia (beyond the scope of this article) has been reported by several authors. For a synthesis of regional geology see Caminos (1999) and references therein. In this work only a summary of the subject is referred to.

The study area is located between the latitudes 40º and 52º S and longitudes 67º and 71º W. These coordinates delimit the Patagonian region, the focus of this work which also includes the southern stretch of the Andes as described in figure (1) where the main pre-Jurassic tectonic elements are the Northern Patagonian and the Deseado Massifs.

In these regions there is a Jurassic rhyolitic volcanic rock domain which forms one of the largest siliceous provinces in the world (Pankhurst et. al., 1998).

The siliceous volcanic field of Patagonia extends from the Atlantic coast to the Chilean Andean region. Eastern Patagonia is geologically divided into stable areas in which the volcanic rocks are now exposed in the Northern and Deseado Patagonian massifs and the intermediate areas covered by the Cretaceous and Tertiary sedimentary rocks of the San Jorge and Magellan Basins (Pankhurst et al 1998). The most important geological units in the region are the Choiyoi complex (Triassic -

Jurassic), the Chon Aike complex (Jurassic - Cretaceous) and the plutonic rocks (Permo - Triassic).

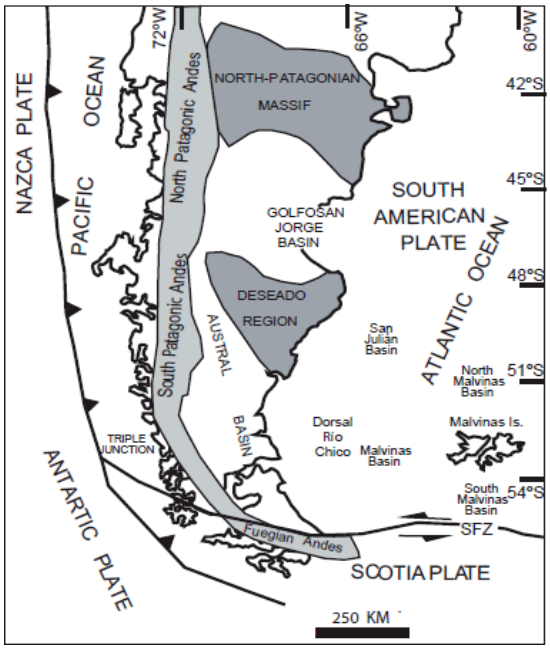


*Figure 1 - Major geological provinces of Patagonia (Giacosa et al., 2012)*

The basement rocks occupy a larger area in the Northern Patagonian Massif. The main types of rocks which occur on the western edge of the massif in Paleozoic granite intrusions are Shales and Gneiss. In the southwestern part of the massif carboniferous and Permian gneisses occur (Pankhurst et al., 1998; 2006).

In the Deseado massif a series of small outcrops occur that reveal sequences of micaceous materials and amphibolitic shales possibly of pre-Cambrian or late Cambrian age Permo-Triassic conglomerates fill small basins and represent the oldest evidence of an extensional regime that became more pronounced during the Triassic period with the regional formation of NNW - SSE trend graben throughout Patagonia (Pankhurst et al., 1998).

### 3. Materials and Methods

Outcrops of xenoliths in the form of alkaline basaltic lavas occur in various areas of Patagonia. Samples from these outcrops were collected by Ntaflos et al., (2006) in the region limited by latitudes 40º and 52ºS and longitudes 67º and 71ºW, occurring in the provinces of Rio Negro, Chubut and Santa Cruz.

Figure (2) shows the occurrences of xenoliths in the provinces of Río Negro, Chubut and Santa Cruz. Argentina. Patagonian xenolith samples include harzburgite spinel, harzburgite garnet, harzburgite spinel, lherzolite spinel, websterite spinel and small quantities of wehrlites dunites and pyroxenites in sizes ranging from 1 and 20 cm (Mallmann, 2004; Bjerg et al., 2005; Ntaflos et al., 2007; Rieck et al., 2007; Schilling et al., 2017 and references therein).

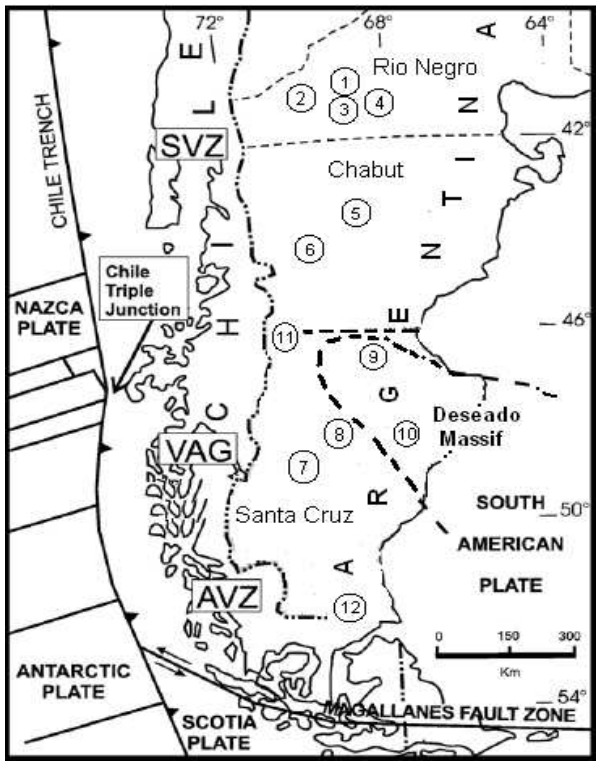


*Figure 2 - Location of mantle xenoliths in Río Negro. Chubut and Santa Cruz provinces (modified from Ntaflos et al, 2007). The abbreviations used are: SVZ - Southern Volcanic Zone; VGZ - Volcanic Gap Zone; AVZ – Austral Volcanic Zone.The numbers correspond to the following localities: 1- Estacia Alvarez; 2- Cerro de Monjon; 3- Prahuaniyeu; 4- Laguna Fria;5- Paso de Indios; 6- Cerro de los Chenques; 7- Tres Lagos; 8- Gobernador Gregores; 9- Cerro Clark; 10- Auvernia; 11- Coyhaique; e 12- Pali Aike.*

Tables (1) and (2) present the pressure and temperature information, as well as the types of dominant minerals present in xenoliths samples in the provinces of Rio Negro and Santa Cruz, compiled from various works as described in the references. Details on the geothermometers and geobarometers used to estimate the pressure and temperature of equilibrium can be consulted in the references from which the information was compiled.

Table 1 - Pressure and Temperature (P-T) data on mantle xenoliths in the Rio de Negro Province.

| P (kb) | T(ºC) | Description | Reference |
|---|---|---|---|
| 11 | 877 | Harzburgito | Mallmann (2004) |
| 14 | 914 | Harzburgito | Mallmann (2004) |
| 14 | 936 | Lherzolito | Mallmann (2004) |
| 15 | 942 | Lherzolito | Mallmann (2004) |
| 16 | 993 | Harzburgito | Mallmann (2004) |

| | | | |
|---|---|---|---|
| 19 | 1079 | Harzburgito | Mallmann (2004) |
| 17 | 1122 | Spinel Harzburgite | Bjerg et. al. (2005) |
| 20 | 1180 | Spinel Harzburgite | Bjerg et. al. (2005) |
| 23 | 1200 | Garnet Lherzolite | Bjerg et. al. (2005) |
| 24 | 1253 | Spinel Harzburgite | Bjerg et. al. (2005) |

Table 2 - Pressure and Temperature (P-T) data on mantle xenoliths in the Santa Cruz Province

| P (kb) | T(ºC) | Description | Reference |
|---|---|---|---|
| 10 | 728 | Spinel Peridotites | Ntaflos et al., (2007) |
| 12 | 830 | Spinel Lherzolite | Bjerg et al., (2005) |
| 13 | 850 | Lherzolite | Schilling et al., (2017) |
| 14 | 884 | Spinel Peridotites | Ntaflos et al., (2007) |
| 15 | 968 | Harzburgite | Schilling et al., (2017) |
| 16 | 1021 | Lherzolite | Schilling et al., (2017) |
| 17 | 1040 | Spinel Peridotites | Ntaflos et al., (2007) |
| 16 | 1055 | Spinel Harzburgite | Bjerg et al., (2005) |
| 16 | 1057 | lherzolite | Schilling et al., (2017) |
| 16 | 1064 | Harzburgite | Schilling et al., (2017) |
| 22 | 1196 | Spinel lherzolite | Bjerg et al., (2005) |
| 24 | 1260 | Garnet Harzburgite | Bjerg et al., (2005) |

## 4. Model Description

Regarding the main mode of heat transfer in the lithosphere is conduction, we can develop a model to estimate the thermal field of the lithosphere from the following parameters: temperature, heat flow, radiogenic heat production and thermal conductivity.

The model proposed in this work is composed of two layers, as described in figure (3). This analysis is similar to that proposed by Russell and Kopylova (1999); Lewis et. al., (2003); Harder and Russell, (2006); and Greenfild et al., (2013).

The layer (1) represents the crust with top on the Earth's surface, where $Z_0$=0 and the base on the top mantle at the $Z_M$ position. In this layer the radiogenic heat production $A_0$ and the thermal conductivity $\lambda_0$ are constant, $T_0$ represents the temperature and $q_0$ the heat flow, both on the surface.

The layer (2) represents the lithospheric mantle. The top of this region is the $Z_M$ position and the base at the $Z_A$ position. $Z_M$ is Moho's depth, this way it also represents the crustal thickness. The radiogenic heat production $A_M$ in layer (2) is assumed to be constant, but thermal conductivity $\lambda(T)$ is a function of temperature, while B is the coefficient of variation of thermal conductivity with temperature. $T_M$ and $q_M$ are respectively the temperature and the heat flow at Moho's depth.

The $Z_A$ position physically represents the thickness of the thermal lithosphere which is the region of the lithosphere by definition, where the main mode of heat transfer is conduction. In this position the temperature $T_A$ has a value of approximately 1300ºC and $q_A$ the heat flow from the asthenosphere.

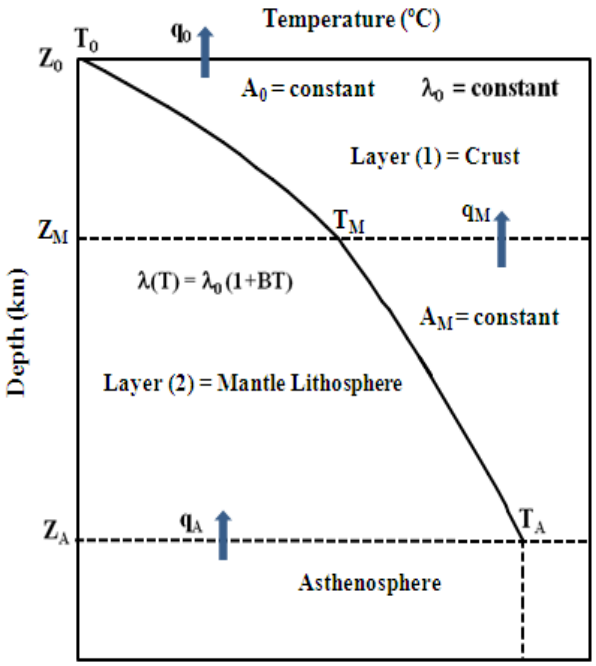


*Fig. 3 - Schematic representation of model for conductive heat transfer in the crust and mantle lithosphere.*

Based on the schematic representation presented in figure (5) we can formulate the temperature distribution in the lithosphere for the layers (1) and (2) from the one-dimensional equation of heat in permanent regime. In these conditions equation (1a) can be considered as representative of the thermal field for layer (1). The equation (1b) and (1c) are the contour conditions. In this layer the thermal conductivity and the radiogenic heat production are assumed to be constant.

$$\frac{d^2T_1}{dZ^2} = -\frac{A_0}{\lambda_0} \qquad Z_0 < Z < Z_M \qquad (1a)$$

$$T_1(Z = Z_0) = T_0 \qquad (1b)$$

$$T_1(Z = Z_M) = T_M \qquad (1c)$$

where $T_1$ represents the temperature and the other variables are those described and informed in item 4. The solution to the boundary value problem described by equations (1a) to(1c) is the one shown in equation (2).

$$T_1(Z) = -\frac{A_0}{2\lambda_0}Z^2 + \left[\left(\frac{T_M - T_0}{Z_M}\right) + \frac{A_0}{2\lambda_0}Z_M\right]Z + T_0 \qquad (2)$$

Equation (2) represents the temperature distribution for the layer (1). The equation (3a) shows the formulation for layer (2). The equation (3b) and (3c) are the boundary conditions and the equation (3d) shows the variation of thermal conductivity with temperature. The radiogenic heat production in this layer is assumed to be constant.

$$\frac{d}{dZ}\left[\lambda(T_2)\frac{dT_2}{dZ}\right] = -A_M \qquad Z_M < Z < Z_A \qquad (3a)$$

$$T_2(Z = Z_M) = T_M \qquad (3b)$$

$$\lambda(T_2)\frac{dT_2}{dZ} = q_M \qquad (3c)$$

$$\lambda(T_2) = \lambda_0(1 + BT_2) \qquad (3d)$$

where $T_2$ represents the temperature and the other variables are those described and informed in item 4. The solution to the boundary value problem described by equations (3a) to (3d) is that presented in equation (4).

$$T_2(Z) = \frac{q_M}{\lambda_0}(Z - Z_M) - \frac{A_M}{2\lambda_0}(Z - Z_M)^2 - \frac{B}{2}[T_2(Z) - T_M]^2 + T_M \qquad (4)$$

The equation (4) represents the temperature distribution for the layer (2). The solution of equation (1) was obtained by applying conventional methods for solving differential equations with these characteristics. The solution of equation (3) was obtained by applying Kirchhoff Transform to remove nonlinearity and consequently transform the nonlinear problem into a linear one (For details see Özisik, 1980). This technique was used by Dipple and Kopylova (2000) and Russel et al., (2001) to determine the production and flow of heat in the region of Slave Craton. Canada. Alexandrino and Hamza (2008) used this technique to estimate the thermal field of the Brazilian geological province of San Francisco.

## 5. Methodology to estimate the geothermal parameters.

In order to use the model proposed in this work is necessary to know some initial information. This information is the one in table (3). $T_0$ is the average annual surface temperature of the study area. Thermal conductivity $\lambda_0$ and density ρ have similar values to those used by Russell and Kopylova (1999), Lewis et al., (2003), Harder and Russell (2006), and Greenfield et al., (2013). According to Chulick et al., (2013) and Lloyd et al., (2010) the crustal thickness $Z_M$ in the Patagonia region is between 28 and 32 km.

Results from numerical simulations indicate that small variations in the value of $Z_M$ do not significantly affect estimates of lithospheric thicknesses. Thus, we assume the average value of 30 km as the characteristic of the crustal thickness of the region.

Table (3) - Physical parameters used in the model

| Property | Lithospheric Layers | |
|---|---|---|
| | Crust | Mantle |
| $T_0$ (ºC) | 10 | --- |
| $Z_M$ (km) | 30 | --- |
| $\lambda_0$ (W m$^{-1}$ ºC$^{-1}$) | 2.5 | 3.0 |
| ρ (kg m$^{-3}$) | 2700 | 3300 |

Below we describe the sequential process to estimate the geothermal parameters of interest:

### 5.1- Geothermal parameters at Moho depth.

To estimate the geothermal parameters at the depth of Moho such as temperature $T_M$, heat flow $q_M$, radiogenic heat production $A_M$ and the coefficient of variation of thermal conductivity with temperature B at the depth of Moho we use the pressure and temperature balance data described in tables (1) and (2) the physical parameters described in table (3) and equation (4) to form a system of equations.

The system of equations formed from temperature and pressure balance data allows us to estimate $T_M$, $q_M$, $A_M$ and B at Moho depth using appropriate numerical methods. In this work we use the RNLIN routine available in IMSL. The RNLIN routine uses a modified Levenberg-Marquardt method.

### 5.2 - Radiogenic heat production in the surface $A_0$.

To estimate the heat production at the surface we derive the equation (2), thus obtaining the equation (5).

$$\frac{dT_1}{dZ}(Z) = -\frac{A_0}{\lambda_0}Z + \left[\left(\frac{T_M - T_0}{Z_M}\right) + \frac{A_0}{2\lambda_0}Z_M\right] \qquad (5)$$

We evaluate the equation (5) at the Z=ZM position and multiply the resulting equation by $\lambda_0$. Following this procedure we arrive at equation (6) and thus we can estimate $A_0$.

$$A_0 = \frac{2}{Z_M}\left[\lambda_0\left(\frac{T_M - T_0}{Z_M}\right) - q_M\right] \qquad (6)$$

### 5.3 - Geothermal heat flow in the surface $q_0$.

To estimate the value of the heat flow at the surface, we multiply the eq. (5) by $\lambda_0$ evaluated at position. $Z=Z_0=0$.

$$q_0 = \lambda_0\left[\left(\frac{T_M - T_0}{Z_M}\right) + \frac{A_0}{2\lambda_0}Z_M\right] \qquad (7)$$

## 6. Results and Discussion

Tables (4) and (5) present the results of geothermal parameter estimates for the provinces of Rio Negro and Santa Cruz. The values of the coefficient of variation of thermal conductivity with temperature and radiogenic heat production in all provinces are compatible with those expected for these parameters (Jaupart and Mareschal, 1999; Kukkonen and Peltonen, 1999; Russell et al., 2001; Artemieva, 2001; Dymshits et al., 2020).

In the province Rio Negro, Table (5) the heat flow varies from 73 to 84 $mWm^{-2}$ and the radiogenic heat production from 1.0 to 1.3 $\mu Wm^{-3}$ in the surface. At Moho's depth the temperature and the heat flow have average values of 750 ºC, 44 $mWm^{-2}$ respectively and 75 km is the value of the thermal thickness of that province. The lowest thermal thickness estimated in this work.

Table 4 - Sumary of model results for geothermal parameters of the Rio Negro province.

| Rio Negro province model parameters | | | | |
|---|---|---|---|---|
| Property | Estimate | | | |
| | Lower | Upper | Best | ± |
| $T_M$ (ºC) | 712 | 788 | 750 | 38 |
| $q_0$ ($mWm^{-2}$) | 73 | 84 | 79 | 5 |
| $q_M$ ($mWm^{-2}$) | 39 | 50 | 44 | 6 |
| $A_0$ ($\mu Wm^{-3}$) | 1,0 | 1,4 | 1,2 | 0,2 |
| $A_M$ ($\mu Wm^{-3}$) | 2.5E-02 | 3.2E-02 | 2.8E-02 | 3.5E-03 |
| B ($W\ m^{-1}\ ºC^{-2}$) | 1.3E-04 | 1.7E-04 | 1.5E-04 | 1.9E-05 |
| $Z_A$ (km) | 65 | 86 | 75 | 11 |

For the province of Santa Cruz, the parameter values are those shown in the table (5). In this province the heat flow varies from 78 to 91 $mWm^{-2}$ and the radiogenic heat production from 1.2 to 1.8 $\mu Wm^{-3}$ in the surface, These are the highest values when compared to the other provinces. At Moho's depth the parameters vary as follows: temperature between 715 and 804 ºC and heat flow from 34 to 47 $mWm^{-2}$. The average thermal thickness estimated for the province was 82 km.

Table 5 - Sumary of model results for geothermal parameters of the Santa Cruz province.

| Santa Cruz province model parameters | | | | |
|---|---|---|---|---|
| Property | Estimate | | | |
| | Lower | Upper | Best | ± |
| $T_M$ (ºC) | 715 | 804 | 760 | 45 |
| $q_0$ ($mWm^{-2}$) | 78 | 91 | 85 | 7 |
| $q_M$ ($mWm^{-2}$) | 34 | 47 | 40 | 7 |
| $A_0$ ($\mu Wm^{-3}$) | 1.2 | 1.8 | 1.5 | 0.3 |
| $A_M$ ($\mu Wm^{-3}$) | 1.9E-02 | 2.7E-02 | 2.5E-02 | 3.8E-03 |
| B ($W\ m^{-1}\ ºC^{-2}$) | 2.7E-04 | 3.7E-04 | 3.5E-04 | 5.3E-05 |
| $Z_A$ (km) | 69 | 98 | 82 | 15 |

The uncertainties in the estimates of the magnitudes listed in tables (4) and (5) come from a number of sources, including uncertainties of $Z_M$ crustal thickness, pressure, temperature and composition of the xenoliths samples listed in tables (1) and (2) as well as the values of thermal conductivity $\lambda_0$.

To minimize these problems a model of radiogenic heat production and constant thermal conductivity in the crust (layer 1 of figure 3) and constant heat production in the lithospheric mantle (layer 2 of figure 3) were chosen in order to reduce the number of variables in the model and consequently obtain more robust results.

Because the value of temperature at the Moho's depth $T_M$ is associated with crustal thickness, and the value of heat flow at the Moho's depth $q_M$ is associated with the value of thermal conductivity, all cases were simulated considering $Z_M$ = 30 km and $\lambda_0$ = 3.0 $W\ m^{-1}\ ºC^{-1}$ in the lithospheric mantle (layer 2, figure 3). Therefore, the quantities $T_M$ and $q_M$ (equation 4), are influenced only by the production of $A_M$ radiogenic heat and the coefficient of variation of thermal conductivity B.

In relation the production of radiogenic heat in the mantle, the global data indicates that the values of this parameter are in the range of $10^{-6} < A_M < 0.06\ \mu Wm^{-3}$. This represents a variation of ± 5.0 ºC in the temperature value $T_M$ and ± 2.0 $Wm^{-2}$ in the value of the heat flow $q_M$.

The parameter B, according to Kukknen and Jõeleht, 1995; Seipold, 1998, Jaupart and Mareschal, 1999; Artemieva et al., 2001; and Seipold, 2001, in the lithospheric mantle their typical values are between $1x10^{-4} < B < 5x10^{-4}\ Wm^{-1}ºC^{-2}$, which causes a variation of ± 10ºC in the $T_M$ temperature value and in the flow of heat $q_M$ this variation is around ± 4.0 $mWm^{-2}$.

The other constraint used to solve equation (4) was to establish a difference between the observed temperature $T_{OBS}$ and $T_{MODEL}$ below or equal to 20ºC. This value was chosen due to the uncertainty in the thermobarometry calibration estimated at ± 20 ºC and ± 0.3 GPa for the geothermometer proposed by Brey and Kohler, 1990.

Figures (4) and (5) show the results of the temperature distribution for the provinces Rio Negro and Santa Cruz. In the figures we can observe the maximum and minimum values of the modeled temperature profiles, as well as the observed data.

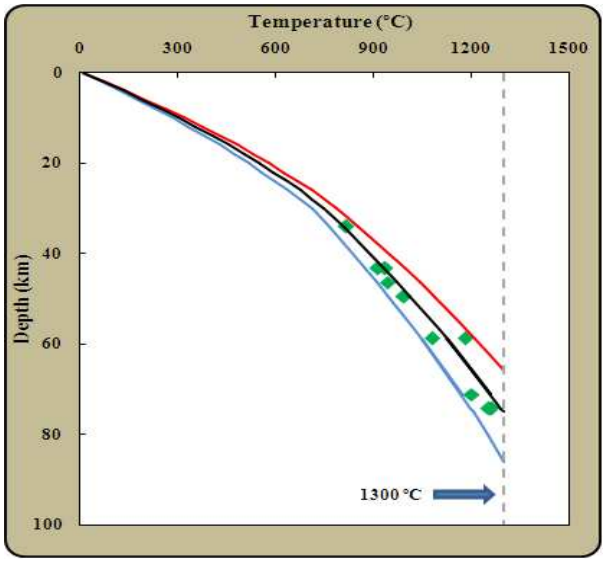


*Figure 4 - temperature distribution of the Rio Negro province, red line represents the upper limits, blue line the lower limit and black line the best fit. The limits were established with 95% confidence. Gray dotted line represents the isotherm of 1300 ºC and the green dots are the observed data.*

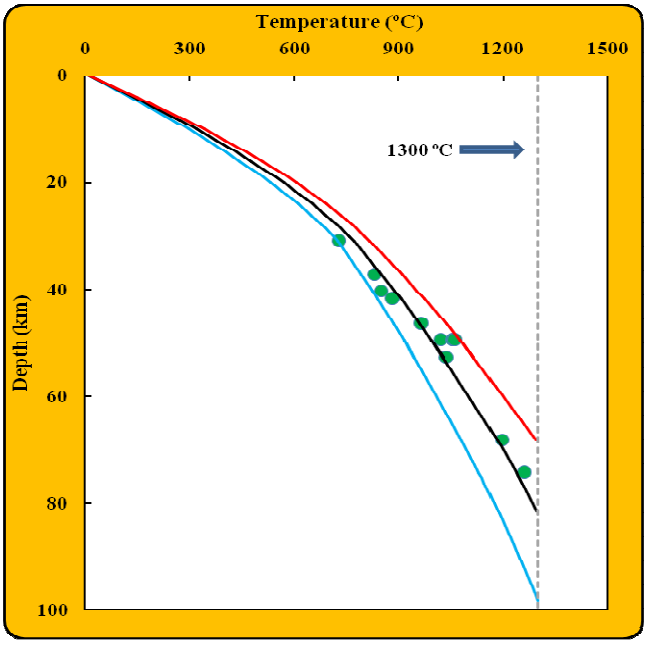


*Figure 5 - temperature distribution of the Santa Cruz province, red line represents the upper limits, blue line the lower limit and black line the best fit. The limits were established with 95% confidence. Gray dotted line represents the isotherm of 1350 ºC and the green dots are the observed data.*

Figure (6) shows that using the strategy of fixing $Z_M$ and $\lambda_0$ and to refine the values of AM and B within the range of expected values for these quantities. It was possible to estimate the variables in equation (4) $T_M$, $A_M$, $q_M$, and B in order to obtain the difference between $T_{OBS}$ and $T_{MODEL}$ within the range of uncertainties of the geothermobarometer.

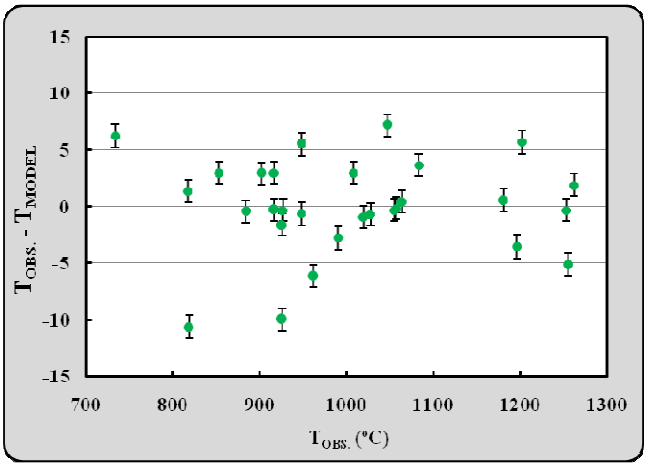


*Figure 6 - Residue (difference between observed and modelled temperature) versus observed temperature. The residues are below 15 ºC.*

Imposing these restrictions, we obtain a good quality of the adjustment, as can be verified by the analysis of figure (7) where we can observe that the correlation coefficient $R^2$ > 0,99 a value that confirms a strong correlation between the observed data and those predicted by the model.

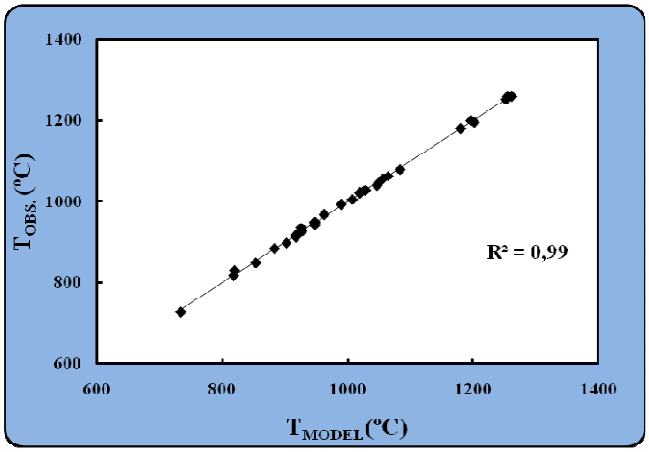


*Figure 7- Relationship between observed and modelled data. The value of $R^2$ shows strong correlation between the linear of the model.*

## 7. Conclusions

Only the best estimated values were considered. We can infer average values for geothermal parameters at the surface: heat flow 81 $mWm^{-2}$, radiogenic heat production 1.4 $\mu Wm^{-3}$ at Moho depth: heat flow 40 $mWm^{-2}$, radiogenic heat production $2x10^{-2}$ $\mu Wm^{-3}$ and temperature 734ºC. Thermal thickness 81km and coefficient of variation of thermal conductivity with temperature $2x10^{-4}$ W $m^{-1}$ $ºC^{-2}$.

The value of heat flow at the surface is similar to those estimated by Vieira and Hamza (2019), Ávila and Dávila, (2018), Cardoso et al., (2010), radiogenic heat production and the parameter of variation of thermal conductivity at Moho's depth are within the range of expected values, so we can consider that the model presents coherent results, which may better show the applications of the model when more accurate data are available.

Santa Cruz province has the highest heat flow at the surface and also the highest temperature value at Moho depth, Río Negro province has the lowest thermal thickness value and the highest heat flow at Moho depth, this indicates that there are possibly two plumes heads responsible for xenoliths deposition in the region: one in Río Negro province and another in Santa Cruz.

## References

Alexandrino, C.H., Hamza, V.M., 2008, Estimates of heat flow and heat production and a thermal model of the São Francisco Cráton. International Journal of Earth Sciences, Volume 97, Number 2, April 2008, pp. 289-306.

Artemieva, I.M. and Mooney, W.D., Thermal Thickness and Evolution of Precambrian Lithosphere: A Global Study, *J. Geophys. Res.*, 2001, vol. 106, no. B8, pp. 16387–16144.

Aulbach, S.; Griffin, W.L.; O'reilly, S.Y.; Mccandles, T.E. Genesis and evolution of the lithospheric mantle beneath the Buffalo Head Terrane, Alberta (Canada). Lithos 2004, 77, 413–451.

Brey, G., Köhler, T. 1990. Geo-thermo-barometry in four-phase lherzolites II. New thermo-barometers, and practical assessment of existing thermo-barometers. Journal of Petrology, 31(6): 1353–1378. doi:10.1093/petrology/31.6.1353.

Bjerg, E.A., Ntaflos, TH., Kurat, G., Dobosi, G., Labudia, C.H., 2005. The upper mantle beneath Patagonia, Argentina, documented by xenoliths from alkali basalts. J. South Am. Earth Sci. 18 (2), 125–142.

Caminos, R., 1999. Geología Argentina, Instituto de Geología y Minería, SEGEMAR, Anales No. 29, Buenos Aires 786 pp.

Chulick,G.S., Detweiler, S.,Mooney, W.D., 2013, Seismic structure of the crust and uppermost.Journal of South American Earth Sciences, 42, 260-276: https://doi.org/10.1016/j.jsames.2012.06.002.

Dymshits, A.M.,Sharygin, I.S.,Malkovets, V.G., Yakovlev, I.V.,Gibsher, A.A.,Alifirova, T.A.,Vorobei, S.S.,Potapov, S.V.,Garanin, V.K., 2020, Thermal State, Thickness, and Composition of the Lithospheric Mantle beneath the Upper Muna Kimberlite Field (Siberian Craton) Constrained by Clinopyroxene Xenocrysts and Comparison with Daldyn and Mirny Fields. *Minerals*, *10*, 549.

Fabio Vieira, Valiya Hamza, 2019, Assessment of Geothermal Resources of South America - A New Look, International Journal of Terrestrial Heat Flow and Applied Geothermics VOL. 2, NO. 1 (2019); P. 46-57. ISSN: 2595-4180, DOI: https://doi.org/10.31214/ijthfa.v2i1.32

Giacosa, R., D. Fracchia and N. Heredia (2012) Structure of the Southern Patagonian Andes at 49°S. Geologica Acta, Vol. 10, Nº 3, September 2021, 265 -282.

Greenfield, A.M.R. Ghent, E.D. Russell, J.K.,2013, Geo-thermo-barometry of spinel peridotites from southern British Columbia: implications for the thermal conditions in the upper mantle. *Canadian Journal of Earth Sciences*; 50 (10): 2013 – 1019 –1032. doi: https://doi.org/10.1139/cjes-2013-0037.

Harder, M., Russell, J.K. 2006, Thermal state of the upper mantle beneath the Northern Cordilleran Volcanic Province (NCVP), British Columbia, Canada. Lithos, 87(1–2): 1–22. doi:10.1016/j.lithos2005.05.002.

Jaupart, C., Mareschal, J. C., 1999, The thermal structure and thickness of continental roots, Lithos, 48, 93– 114.

Kukkonen, I.T., Peltonen, P. 1999, Xenolith-controlled geotherm for the central Fennoscandian Shield: implications for lithosphere-asthenosphere relations. Tectonophysics, 304: 301–315. doi:10.1016/S0040-1951(99)00031-1.

Lloyd, S., S. van der Lee, G. S. França, M. Assumpção, and M. eng (2010), Moho map of South America from receiver functions and surface waves, J. Geophys. Res., 115, B11315, doi:10.1029/2009JB006829.

Mallmann, G. Processos e componentes mantélicas no Norte da Patagônia (Argentina) e relações com a subducção Andina: evidências petrográficas, geoquímicas e isotópicas em xenólitos ultramáficos mantélicos, 2004, 103 f. Dissertação (Mestrado) - Instituto de Geociências, Universidade Federal do Rio Grande do Sul, Porto Alegre, 2004.

Norberto Rieck JR., Rommulo Vieira Conceição, EdineiKoester, Celine Dantas., 2007, O Manto Litosférico Continental na Região do Cerro de Los Chenques, Argentina: Evidências de Heterogeneidade e Metassomatismo. Geol. USP Sér. Cient., São Paulo, v. 7, n. 1, p. 1-17.

Pilar Ávila, Federico M. Dávila , Heat flow and lithospheric thickness analysis in the Patagonian asthenospheric windows, southern South America. Tecto (2018), doi:10.1016/j.tecto.2018.10.006.

Pankhurst, R. J., Rapela, C. W. Fanning C.M., Márquez, M. 2006,Gondwanide continental collision and the origin of Patagonia. Earth-Science Reviews, 76, 235–257.

Rieck JR., N., Conceição, R., Koester, E., Dantas, C., 2007, O manto litosférico continental na região do Cerro de Los Chenques, Argentina: evidências de heterogeneidade e metassomatismo,.Geologia USP. Série Científica, 7(1), 1-17. https://doi.org/10.5327/Z1519-874x2007000100001.

Rudnick, R.L.,McDonough,W.F.; O'Connell, R.J., Thermal structure, thickness and composition of continental lithosphere. Chem. Geol. 1998, 145, 395–411.

Russell, J.K., Kopylova, M.G., 1999, A steady-state conductive geotherm for the North-central Slave: Inversion of petrological data from the Jericho kimberlite pipe. Journal of Geophysical Research, 104: 7089–7101. doi:10.1029/1999JB900012.

Russell, J.K., Dipple, G.M., Kopylova, M.G., 2001, Heat production and heat flow in the mantle lithosphere to the Slave craton, Canada. Physics of the Earth and Planetary Interiors, 123: 27–44. doi:10.1016/S0031-9201(00)00201-6.

Schilling, M., Carlson, R., Tassara, A., Conceição, R., Bertotto, G., Vásquez Navarro, M., Muñoz Olguín, D., Jalowitzki, T., Gervasoni, F. y Morata Céspedes, D. (2017-06).The origin of Patagonia revealed by Re-Os systematics of mantle xenoliths. Disponible en http://repositorio.uchile.cl/handle/2250/147007.